

1 Introduction to Density Functional Theory

Xavier Blase

Institut Néel

CNRS, Grenoble, France

Contents

1	Overview	2
2	The many-body problem (selected considerations)	3
2.1	One and two-body operators act on the charge and pair density	4
2.2	Exchange-correlation hole and its sum-rule	4
3	Density functional theory	5
3.1	Hohenberg and Kohn theorems	5
3.2	The Euler-Lagrange equation: a density-only formulation	7
3.3	Kinetic-energy functionals: from hydrogen to the HEG	8
3.4	Kohn-Sham formulation: introducing auxiliary 1-body orbitals	9
4	Exchange-correlation functionals	10
4.1	The local density approximation: Ceperley and Alder QMC data	10
4.2	Structural properties within LDA: average impressive results	11
4.3	LDA satisfies the exchange-correlation sum-rule	13
4.4	Jacob's ladder of functionals: towards accuracy heaven?	14
5	On the meaning of Kohn-Sham auxiliary 1-body eigenstates	17
5.1	The band gap problem with DFT Kohn-Sham eigenvalues	18
5.2	Level ordering and self-interaction problems	19
5.3	What is the meaning of Kohn-Sham eigenvalues?	20
5.4	Janak theorem and fractional occupations in ensemble DFT	21

1 Overview

We present in this Chapter a brief overview of Density Functional Theory (DFT), an exact mean-field formalism for calculating ground-state total energies and charge densities. Several excellent books are devoted to DFT and two are listed in the bibliography [1, 2]. At the heart of DFT lies the idea that there is no need to know the details of the many-body wavefunction to calculate ground-state properties: the knowledge of the electronic density $\rho(\mathbf{r})$, a simple 3D scalar function, is enough to obtain the total energy of the system and all quantities that result (atomic structures, binding or atomization energies, elastic constants, phonon energies, activation barriers, the forces needed for molecular dynamics simulations, etc.) As an exact theorem, DFT applies to simple Fermi-liquid-like systems but also to strongly correlated materials.

Unfortunately, the DFT does not say how exactly the ground-state total energy depends on the ground-state electronic density. In practice, approximations are needed to express the kinetic energy and the many-body electron-electron interaction as a “functional” of $\rho(\mathbf{r})$. One thus leaves exact DFT and enters the difficult world of approximations with their specific range of validity. Here comes a second remarkable feature of DFT, namely that very simple approximations for such functionals, including the local density approximation (LDA), deliver excellent results, such as interatomic bond lengths within 1% of experimental data for a very large number of systems. Such an accuracy, combined with the simplicity of DFT that allows to study systems comprising several hundred atoms, can explain the formidable success of DFT in terms of the number of users and systems studied, with the development of very efficient and easy-to-use codes. This success can certainly contribute to explain that the 1998 Chemistry Nobel prize was awarded to Walter Kohn (and John Pople) for the development of DFT.

It remains, however, that DFT in its original formulation is limited to ground-state properties. As such, the field of electronic excitations, and in particular charged excitations as measured in a photoemission experiment for establishing “band-structures” does not formally lie within the reach of DFT. Fortunately, and unfortunately, a specific implementation of DFT, the Kohn-Sham formalism, introduces auxiliary one-body eigenstates and eigenvalues that are very widely used to calculate electronic energy levels. The rationale for doing so is not firmly established, but very valuable information about band dispersions, orbital shapes, etc. are usually obtained for “not-strongly-correlated” systems. Specific limitations are well established (too small band gaps, underbinding of localized states, etc.) that may find a partial cure by considering “generalized DFT” namely a mean-field approach combining DFT and Hartree-Fock: this is the field of hybrid functionals.

Clearly, there is the need for more solid foundations allowing, to build a formal link between DFT and excited states. This is where we stand nowadays, with a healthy competition between the world of DFT, attempting to bridge the gap with excited states properties, and other approaches that abandon mean-field techniques to tackle the explicit many-body problem, but at a cost that needs to be improved to compete in the study of large systems. This will be the subject of most of the other chapters in this book.

2 The many-body problem (selected considerations)

We start this chapter with a short reminder of quantum mechanics for many-particle (electrons) systems. The quantum states of an N -electron system are described by a wavefunction: $\psi(\mathbf{r}_1\sigma_1, \mathbf{r}_2\sigma_2, \dots, \mathbf{r}_N\sigma_N)$ with \mathbf{r}_i and σ_i space and spin variables. The probability to find N electrons with spins $(\sigma_1, \dots, \sigma_N)$ in the infinitesimal volume $d\mathbf{r}_1 d\mathbf{r}_2 \dots d\mathbf{r}_N$ centered at $\mathbf{r}_1, \mathbf{r}_2, \dots, \mathbf{r}_N$ is given by $d^{3N}\mathcal{P} = |\psi(\mathbf{r}_1\sigma_1, \mathbf{r}_2\sigma_2, \dots, \mathbf{r}_N\sigma_N)|^2 d\mathbf{r}_1 d\mathbf{r}_2 \dots d\mathbf{r}_N$. By definition, the electron density can be found by integrating over $N-1$ spacial-variables and summing over all spins

$$\rho(\mathbf{r}) = N \int d\sigma dx_2 \dots dx_N |\psi(\mathbf{r}\sigma, x_2, \dots, x_N)|^2 \quad \text{where } x_i = (\mathbf{r}_i, \sigma_i)$$

with $\rho(\mathbf{r})d\mathbf{r}$ the number of electrons in the infinitesimal volume $d\mathbf{r}$ centered at \mathbf{r} . From the normalization of ψ one obtains $\int d\mathbf{r} \rho(\mathbf{r}) = N$. The charge density can be obtained by multiplying by the elementary charge ($-e$). Note that it is customary to use the wording charge density for electron density.

The electronic Hamiltonian is actually known (atomic units):

$$\hat{H} = -\frac{1}{2} \sum_{i=1}^N \nabla_i^2 + \sum_{i=1}^N v^{\text{ion}}(\mathbf{r}_i) + \sum_{i<j} \frac{1}{|\mathbf{r}_i - \mathbf{r}_j|} \quad \text{with } v^{\text{ion}}(\mathbf{r}) = - \sum_I \frac{Z_I}{|\mathbf{R}_I - \mathbf{r}|} \quad (1)$$

where we did not include the kinetic energy of the ions. v^{ion} is the ionic potential acting on electrons with $\{\mathbf{R}_I, Z_I\}$ the nuclear positions and charges. The energy of the system is given by the ‘‘expectation value’’ of the Hamiltonian (let’s forget spin)

$$\langle \psi | \hat{H} | \psi \rangle = \int \dots \int d\mathbf{r}_1 d\mathbf{r}_2 \dots d\mathbf{r}_N \psi^*(\{\mathbf{r}_i\}) \hat{H}(\{\mathbf{r}_i\}, \{\nabla_{\mathbf{r}_i}\}) \psi(\{\mathbf{r}_i\}).$$

As such, it may seem that quantum mechanics is easy, with first-principles equations and formalisms developed in the first half of the 20th century. Let’s consider, however, the energy of a very small system, the water molecule with its 10 electrons. Let’s assume that we want to calculate its total energy for some wavefunction ψ (let’s not even ask how we obtained it ...) Applying naively some quadrature (e.g. trapezoidal rule) to calculate such an integral by paving the space around the molecule with a coarse $10 \times 10 \times 10$ grid, one obtains for $N=10$ electrons a sum of $10^{3N} = 10^{30}$ terms to calculate and add. Modern computers are ‘‘petaflop’’: they perform 10^{15} floating point operations per second. We would therefore need of the order of 10^{15} seconds, namely 31 710 millennia for this simple evaluation! Clearly, the way we calculated this integral was very dumb, and clever sampling of phase space can be done much more efficiently using, e.g., Metropolis sampling. It remains that the exact many-body problem becomes dramatically expensive as soon as the number of electrons increases. Computers are handy, but the brains of the physicists and chemists to come up with nice approximations are luckily still required.

We now start by introducing simple considerations demonstrating that one does not always need all the details of the complex many-body wavefunction to calculate a physical observable. Unless stated otherwise, we will not display spin variables in the following for sake of brevity of the equations.

2.1 One and two-body operators act on the charge and pair density

Let us consider one-body operators, namely operators of the form $\hat{O} = \sum_{i=1}^N O(\mathbf{r}_i)$, where the $\{\mathbf{r}_i\}$ are the electronic positions. In particular, the electron-ion interaction energy is given by $E^{\text{ion-e}} = \sum_i \langle \psi | v^{\text{ion}}(\mathbf{r}_i) | \psi \rangle$ with

$$\begin{aligned} \langle \psi | v^{\text{ion}}(\mathbf{r}_i) | \psi \rangle &= \int d\mathbf{r}_1 d\mathbf{r}_2 \dots d\mathbf{r}_N v^{\text{ion}}(\mathbf{r}_i) |\psi(\mathbf{r}_1, \mathbf{r}_2, \dots, \mathbf{r}_i, \dots, \mathbf{r}_N)|^2 \\ &= \int d\mathbf{r} d\mathbf{r}_2 \dots d\mathbf{r}_N v^{\text{ion}}(\mathbf{r}) |\psi(\mathbf{r}, \mathbf{r}_2, \dots, \mathbf{r}_N)|^2 \end{aligned}$$

where we have renamed all variables, in particular $\mathbf{r}_i \Rightarrow \mathbf{r}$, and reshuffled all space positions thanks to the symmetry properties of $|\psi|^2$. As a result, all N terms are identical, yielding

$$E^{\text{ion-e}} = N \int d\mathbf{r} v^{\text{ion}}(\mathbf{r}) \int d\mathbf{r}_2 \dots d\mathbf{r}_N |\psi(\mathbf{r}, \mathbf{r}_2, \dots, \mathbf{r}_N)|^2 = \int d\mathbf{r} v^{\text{ion}}(\mathbf{r}) \rho(\mathbf{r}).$$

As such, v^{ion} acts only on the electronic (or charge) density: there is no need for the full many-body wavefunction and its related $3N$ -integrals to get the $E^{\text{ion-e}}$ energy!

To conclude this paragraph, one can introduce another one-body operator, the electron density operator, $\hat{\rho}(\mathbf{r}) = \sum_{i=1}^N \delta(\mathbf{r} - \mathbf{r}_i)$, that ‘‘counts’’ the number of electrons at \mathbf{r} . The same demonstration as above (exercise!) allows to recover the expression for the electronic density: $\rho(\mathbf{r}) = \langle \psi | \hat{\rho}(\mathbf{r}) | \psi \rangle = N \int d\mathbf{r}_2 \dots d\mathbf{r}_N |\psi(\mathbf{r}, \mathbf{r}_2, \dots, \mathbf{r}_N)|^2$.

Let’s now consider the crucial case of two-body operators. The electron-electron interaction energy $E^{ee} = \langle \psi | \hat{V}^{ee} | \psi \rangle$ with $\hat{V}^{ee} = \sum_{i < j}^N \frac{1}{|\mathbf{r}_i - \mathbf{r}_j|}$ can also be simplified by renaming and reshuffling the integration variables:

$$\langle \psi | \frac{1}{|\mathbf{r}_i - \mathbf{r}_j|} | \psi \rangle = \int d\mathbf{r} d\mathbf{r}' d\mathbf{r}_3 \dots d\mathbf{r}_N \frac{|\psi(\mathbf{r}, \mathbf{r}', \mathbf{r}_3, \dots, \mathbf{r}_N)|^2}{|\mathbf{r} - \mathbf{r}'|}$$

independent of the specific (i, j) indices, yielding $N(N-1)/2$ identical terms so that $E^{ee} = \int d\mathbf{r} d\mathbf{r}' \rho_2(\mathbf{r}, \mathbf{r}') / |\mathbf{r} - \mathbf{r}'|$ with

$$\rho_2(\mathbf{r}, \mathbf{r}') = \frac{N(N-1)}{2} \int d\mathbf{r}_3 \dots d\mathbf{r}_N |\psi(\mathbf{r}, \mathbf{r}', \mathbf{r}_3, \dots, \mathbf{r}_N)|^2$$

which is the density of pairs satisfying $\int d\mathbf{r} d\mathbf{r}' \rho_2(\mathbf{r}, \mathbf{r}') = N(N-1)/2$.

For calculating the complex electron-electron energy responsible for electronic correlations, there is no need, in principle, for all the details of the many-body wavefunctions and the related $3N$ -integrals: we only need averaged (mean-field) quantities such as the 2-body pair-density! BUT we do not know at this stage how to build $\rho_2(\mathbf{r}, \mathbf{r}')$ without the knowledge of ψ .

2.2 Exchange-correlation hole and its sum-rule

Rewriting the pair density as $2\rho_2(\mathbf{r}, \mathbf{r}') = \rho(\mathbf{r})\rho(\mathbf{r}') [1 + h(\mathbf{r}, \mathbf{r}')]]$, with h called the pair-correlation function, one can express E^{ee} in terms of the (charge-charge) Hartree energy J

$$J = \frac{1}{2} \int d\mathbf{r} d\mathbf{r}' \frac{\rho(\mathbf{r})\rho(\mathbf{r}')}{|\mathbf{r} - \mathbf{r}'|}$$

and the exchange-correlation (XC) hole density $\rho_{XC}(\mathbf{r}, \mathbf{r}') := \rho(\mathbf{r}')h(\mathbf{r}, \mathbf{r}')$ as

$$E^{ee} = J + \frac{1}{2} \int d\mathbf{r}d\mathbf{r}' \frac{\rho(\mathbf{r})\rho_{XC}(\mathbf{r}, \mathbf{r}')}{|\mathbf{r} - \mathbf{r}'|}.$$

It is easy to demonstrate (exercise!) that

$$\int d\mathbf{r}' \rho_2(\mathbf{r}, \mathbf{r}') = \frac{N-1}{2} \rho(\mathbf{r}) \quad \text{and} \quad \int d\mathbf{r}' \rho_{XC}(\mathbf{r}, \mathbf{r}') = -1$$

yielding the XC-hole sum rule. The XC energy is the Coulomb energy between electrons and their respective XC-hole, namely the depletion of the charge density by one electron (through exchange and Coulomb repulsion) dynamically created around each electron. The 1/2 in the XC energy is an adiabatic factor: the XC hole grows with the electron density and would not exist without it.

The XC energy beyond the classical Hartree term can be written in a classical form as the Coulomb interaction between an electron and its XC hole, namely the dynamical depletion of exactly one charge created “locally” by Fermi and Coulomb repulsion. Due to the XC sum rule, the composite object (a quasiparticle) made out of the electron dressed by its XC hole is a neutral object weakly interacting with its surrounding. Independent-like particle theories, and related 1-body eigenvalue equations, are therefore more likely to be successful when applied to such quasiparticles.

3 Density functional theory

We have established that we do not need to know all the details of the many-body wavefunction to obtain in particular the electron-electron interaction energy. The pair density is sufficient. It can be shown further that the kinetic energy can be obtained from the knowledge of the 1st-order density matrix: $\gamma_1(\mathbf{r}, \mathbf{r}') = N \int \cdots \int d\mathbf{r}_2 \cdots d\mathbf{r}_N \psi(\mathbf{r}, \mathbf{r}_2, \cdots, \mathbf{r}_N) \psi^*(\mathbf{r}', \mathbf{r}_2, \cdots, \mathbf{r}_N)$ which is also a 2-body function averaging out most of the many-body wavefunction degrees of freedom. Density Functional Theory (DFT) goes one step beyond, demonstrating that the ground-state (GS) total energy only requires the knowledge of the electronic density, very much as for the action of the one-body ionic potential.

3.1 Hohenberg and Kohn theorems

Preliminaries: Room temperature is of the order of 25 meV, much smaller than typical electronic energy gaps or band dispersions, so most unperturbed (no strong light, etc.) solids or molecules are close to their lowest energy state with wavefunction ψ_{GS} and energy E_{GS} .

The variational principle provides a way to find ψ_{GS} and energy E_{GS} :

$$E_{GS} = \min_{\psi} E[\psi] \quad \text{with} \quad E[\psi] = \langle \psi | \hat{H} | \psi \rangle \quad \text{and} \quad \langle \psi | \psi \rangle = 1$$

This is the standard approach, where the energy is a *functional* of the many-body wavefunction ψ . The dramatic result from Hohenberg and Kohn [3] is that the ground-state energy can be written as a functional of the charge density:

$$E_{GS} = \min_{\psi} E[\psi] \xrightarrow{DFT} E_{GS} = \min_{\rho} E[\rho] \quad \text{with} \quad \int d\mathbf{r} \rho(\mathbf{r}) = N.$$

This is an *exact* result, namely there is an exact mean-field theory for the problem of the ground-state energy in N -electron systems!

Demonstration for non-degenerate ground-states: The ionic potential acts on the charge density and the electronic Hamiltonian (without ion-ion interaction) reads

$$\hat{H} = \hat{T} + \hat{V}^{ee} + \int d\mathbf{r} v^{ext}(\mathbf{r})\rho(\mathbf{r})$$

with \hat{T} the kinetic energy and $v^{ext}=v^{ion}$ (the ions are “external” to the N -electron system).

Theorem: given a charge density $\rho(\mathbf{r})$, then there exist only one external potential $v^{ext}(\mathbf{r})$ (within a constant) such that the corresponding ground-state electronic density is equal to $\rho(\mathbf{r})$.

Reductio ad absurdum: Assume there exist 2 external potentials $v_1^{ext}(\mathbf{r})$ and $v_2^{ext}(\mathbf{r})$ that lead to the same ground-state charge density:

$$\begin{aligned} v_1^{ext}(\mathbf{r}) &\implies \hat{H}_1 \implies \psi_1^{GS} \implies \rho(\mathbf{r}) \\ v_2^{ext}(\mathbf{r}) &\implies \hat{H}_2 \implies \psi_2^{GS} \implies \rho(\mathbf{r}) \end{aligned}$$

Using the variational principle

$$\begin{aligned} E_1^{GS} = \langle \psi_1 | \hat{H}_1 | \psi_1 \rangle &< \langle \psi_2 | \hat{H}_1 | \psi_2 \rangle = \langle \psi_2 | \hat{H}_2 | \psi_2 \rangle + \langle \psi_2 | \hat{H}_1 - \hat{H}_2 | \psi_2 \rangle \\ &= E_2^{GS} + \int d\mathbf{r} (v_1^{ext} - v_2^{ext})(\mathbf{r})\rho(\mathbf{r}) \end{aligned}$$

Starting now from $\langle \psi_2 | \hat{H}_2 | \psi_2 \rangle$ (switching indices 1 and 2) one obtains

$$E_2^{GS} < E_1^{GS} + \int d\mathbf{r} (v_2^{ext} - v_1^{ext})(\mathbf{r})\rho(\mathbf{r})$$

and by adding the two inequalities

$$E_1^{GS} + E_2^{GS} < E_2^{GS} + E_1^{GS} \quad \text{IMPOSSIBLE!}$$

The demonstration hinges here on strict inequalities, namely assuming non-degenerate ground-states. This is the celebrated 1964 theorem by Hohenberg and Kohn [3].

Ground-state energy as a functional of the charge density: It follows that the charge density completely determines the external potential and thus the Hamiltonian (just add the universal kinetic \hat{T} and V^{ee} operators) and thus the ground-state wavefunction ψ_{GS} :

$$\begin{array}{ccccccc} v^{ext} & \longrightarrow & \hat{H} & \longrightarrow & \psi_{GS} & \longrightarrow & \rho(\mathbf{r}) \\ \uparrow & & & & & & \downarrow \\ & & & & & & \end{array}$$

Since $\rho(\mathbf{r})$ determines ψ_{GS} , it determines unequivocally the total energy of the ground-state, $E_{GS} = \langle \psi_{GS} | \hat{H} | \psi_{GS} \rangle$. It can be shown further as a corollary (Exercise) that the *variational principle* can be now used for E_{GS} as a functional of the charge density:

$$E_{GS} = \min_{\psi} E[\psi] \xrightarrow{DFT} E_{GS} = \min_{\rho} E[\rho] \quad \text{under the constraint that } \int d\mathbf{r} \rho(\mathbf{r}) = N.$$

Since the electron-ion interaction energy can be written explicitly as a functional of the charge density, one concludes that the sum of the kinetic and electron-electron interaction energy is also a functional of $\rho(\mathbf{r})$ that is labeled the universal Hohenberg and Kohn functional $F_{HK}[\rho]$ with $F_{HK}[\rho] = E_{GS}[\rho] - \int d\mathbf{r} v^{\text{ion}}(\mathbf{r})\rho(\mathbf{r})$. It is called universal since, contrary to the ionic potential that depends on the system of interest via the ionic charges and positions, the kinetic energy and electron-electron operators do not.

The basic ideas discussed in this section can be generalized without imposing the non-degeneracy of the ground state, bypassing further the problem of the v -representability of a given density $\rho(\mathbf{r})$: can we always find some v^{ext} potential that leads to a given $\rho(\mathbf{r})$? This can be done within the framework of Levy constrained-search formulation [4] that leads to the following definition for the universal Hohenberg and Kohn functional

$$F_{HK}[\rho] = \min_{\psi \rightarrow \rho} \langle \psi | \hat{T} + \hat{V}^{ee} | \psi \rangle$$

This is formally the standard search over many-body wavefunctions, but with the constraint that for a given density ρ , the search is restricted to many-body wavefunctions with $\langle \psi | \hat{\rho}(\mathbf{r}) | \psi \rangle = \rho(\mathbf{r})$. This further allows to define a kinetic energy and electron-electron interaction energy as independent functionals of the charge density: $T[\rho] = \min_{\psi \rightarrow \rho} \langle \psi | \hat{T} | \psi \rangle$ and $E^{ee}[\rho] = \min_{\psi \rightarrow \rho} \langle \psi | \hat{V}^{ee} | \psi \rangle$.

3.2 The Euler-Lagrange equation: a density-only formulation

The existence of $E[\rho]$ with an associated variational principle allows performing energy minimization with respect to the density under the constraint that the densities we consider integrate to the total number of electrons N . We thus introduce the Lagrangian

$$\Omega[\rho, \mu] = E[\rho] + \mu \left(N - \int d\mathbf{r} \rho(\mathbf{r}) \right)$$

where μ is a Lagrange parameter ensuring the conservation of the correct electron number. This leads by differentiation to the stationary equation

$$\frac{\partial \Omega[\rho, \mu]}{\partial \rho(\mathbf{r})} = 0 \quad \implies \quad \frac{\partial F_{HK}[\rho]}{\partial \rho(\mathbf{r})} + v^{\text{ion}}(\mathbf{r}) = \mu$$

which is a simple 3D differential equation. Its solution is the ground-state charge density from which the ground-state energy of the system can be calculated. This is dramatically simpler than the original many-body wave-function formulation. Unfortunately, we just do not know the universal functional $F_{HK}[\rho]$ expressing the kinetic energy and electron-electron interaction as a function of the density. While functionals of the density for the electron-electron interaction will be discussed and have met much success, one complicated issue remains, the kinetic energy for which we provide now two limiting expressions.

3.3 Kinetic-energy functionals: from hydrogen to the HEG

The first case is the well-known non-interacting homogeneous electron gas (the free-electron gas) that obeys the following relations (see e.g. Kittel)

$$T = \frac{3}{5}N\varepsilon_F \quad \text{with} \quad \varepsilon_F = \frac{\hbar^2 k_F^2}{2m_e} \quad \text{and} \quad k_F^3 = 3\pi^2 \frac{N}{V},$$

where V is the volume occupied by the N electrons, E_F the Fermi energy and T the total kinetic energy. In a homogeneous system, N/V is just the electronic density. It is traditional to rewrite

$$T = \frac{1.105}{r_s^2} \text{ (a.u.)} \quad \text{with} \quad \frac{4}{3}\pi r_s^3 = \frac{V}{N} = \frac{1}{\rho} \quad \text{the Wigner-Seitz radius.}$$

One may then “cook-up” some kinetic energy per electron

$$t_{TF}(\rho) = \frac{T}{N} = \frac{3}{5} \times \frac{\hbar^2}{2m_e} \times (3\pi^2 \rho)^{2/3}$$

yielding the historical Thomas-Fermi (TF) kinetic energy functional approximation for inhomogeneous systems with position dependent densities $\rho(\mathbf{r})$

$$T_{TF} = \int d\mathbf{r} \rho(\mathbf{r}) t^{TF}(\rho(\mathbf{r})) \simeq 2.871 \int d\mathbf{r} \rho(\mathbf{r})^{5/3} \text{ (a.u.)},$$

which is the first example of a local functional: the local kinetic energy density only depends on the density at the same space point. Numerical tests have shown that such an approximation is rather poor for real systems.

Another exact relation can be obtained for the hydrogen atom. In that case, the only occupied orbital is the $1s$ orbital: $\phi(\mathbf{r}) = Ae^{-r}$ (r in a.u.) with A some normalizing constant taken to be positive. Since there is only one electron, the density reads $\rho(\mathbf{r}) = |\phi(\mathbf{r})|^2$. As such

$$T = -\frac{1}{2} \int d\mathbf{r} \phi(\mathbf{r}) \nabla^2 \phi(\mathbf{r}) = \frac{1}{2} \int d\mathbf{r} (\nabla \phi(\mathbf{r})) \cdot (\nabla \phi(\mathbf{r})),$$

where we used integration by part with the wavefunction cancelling at infinity. Using now $\phi(\mathbf{r}) = \sqrt{\rho(\mathbf{r})}$, with $\rho(\mathbf{r})$ positive, we obtain

$$T = \frac{1}{2} \int d\mathbf{r} (\nabla \sqrt{\rho(\mathbf{r})})^2 = \frac{1}{2} \int d\mathbf{r} \left(\frac{\nabla \rho(\mathbf{r})}{2\sqrt{\rho(\mathbf{r})}} \right)^2 = \frac{1}{8} \int d\mathbf{r} \frac{[\nabla \rho(\mathbf{r})]^2}{\rho(\mathbf{r})}.$$

This expression, called the von Weizsäcker functional, is yet another exact formula valid for a given specific system, but clearly very different from the one given above for the homogeneous gas. Anticipating the “gradient corrected functionals” we see that here the energy depends on the density and its gradient.

The search for a universal functional for the kinetic energy turns to be much more challenging than finding a decent functional for the electron-electron interaction. As such, “orbital-free” DFT, namely a DFT based exclusively on the density, has not yet met much success despite its remarkable simplicity.

3.4 Kohn-Sham formulation: introducing auxiliary 1-body orbitals

To bypass this problem of the expressing the kinetic energy as a functional of the density, Kohn and Sham introduced in 1965 their famous approach [5]. The idea goes as follows: in the case of a non-interacting electron system, electronic states can be described by one-body orbitals $\{\phi_n(\mathbf{r})\}$ arranged and populated by increasing energies $\{\varepsilon_n\}$. For such systems, the kinetic energy and electronic density are easily calculated

$$T_0 = -\frac{1}{2} \sum_{n=1}^N \int d\mathbf{r} \phi_n^*(\mathbf{r}) \nabla^2 \phi_n(\mathbf{r}) \quad \text{and} \quad \rho(\mathbf{r}) = \sum_{n=1}^N |\phi_n(\mathbf{r})|^2.$$

Can one imagine now a fictitious non-interacting electron gas submitted to an effective external potential $v^{\text{eff}}(\mathbf{r})$ such that its charge density is the same as that of the real interacting system? Since the ground-state electronic density fulfills the Euler-Lagrange equation, the real and fictitious systems should have the same Euler-Lagrange equation in each point, namely

$$\frac{\partial F_{HK}[\rho]}{\partial \rho(\mathbf{r})} + v^{\text{ion}}(\mathbf{r}) = \frac{\partial T_0}{\partial \rho(\mathbf{r})} + v^{\text{eff}}(\mathbf{r}),$$

yielding the definition of such an effective potential

$$v^{\text{eff}}(\mathbf{r}) = v^{\text{ion}}(\mathbf{r}) + \frac{\partial(F_{HK}[\rho] - T_0)}{\partial \rho(\mathbf{r})}.$$

Introducing the classical (Hartree) charge-charge interaction potential

$$v^H(\mathbf{r}) = \frac{\partial J[\rho]}{\partial \rho(\mathbf{r})} = \int d\mathbf{r}' \frac{\rho(\mathbf{r}')}{|\mathbf{r} - \mathbf{r}'|}$$

with

$$J[\rho] = \frac{1}{2} \int d\mathbf{r} d\mathbf{r}' \frac{\rho(\mathbf{r})\rho(\mathbf{r}')}{|\mathbf{r} - \mathbf{r}'|}$$

one can write

$$v^{\text{eff}}(\mathbf{r}) = v^{\text{ion}}(\mathbf{r}) + v^H(\mathbf{r}) + \frac{\partial E_{XC}[\rho]}{\partial \rho(\mathbf{r})}$$

with E_{XC} the DFT exchange-correlation energy

$$E_{XC} = T[\rho] - T_0[\rho] + E^{ee}[\rho] - J[\rho].$$

We observe that $T[\rho]$ and $E^{ee}[\rho]$ are still to be determined, but the standard argument is that $T_0[\rho]$ captures a significant fraction of $T[\rho]$ so that an approximation performed on E_{XC} is likely to have less detrimental effects as compared to directly approximating $T[\rho]$. We observe that within DFT, the exchange-correlation energy contains some correction to the kinetic energy, not solely the deviation ($E^{ee}[\rho] - J[\rho]$) from the electron-electron interaction to the classical Hartree term. Yet, what is the functional $E_{XC}[\rho]$?

4 Exchange-correlation functionals

The search for exchange-correlation functionals is the central on-going challenge within DFT with decades of failures and difficult successes. Below, we very briefly review some key considerations and terminology.

4.1 The local density approximation: Ceperley and Alder QMC data

Proposed in the seminal 1964 Hohenberg and Kohn paper, the local density approximation (LDA), reminiscent of the Thomas-Fermi kinetic energy functional described above, relies on the following approximation

$$E_{XC}[\rho] \simeq \int d\mathbf{r} \rho(\mathbf{r}) e_{XC}(\rho(\mathbf{r}))$$

where it is assumed that the exchange-correlation energy per electron, $e_{XC}(\mathbf{r})$, for an electron located in \mathbf{r} only depends on the local value of the electronic density $\rho(\mathbf{r})$. Such an approximation is strictly valid only in the limit of a homogeneous electron gas. The next step was then taken by Ceperley and Alder [6] in 1986, who performed nearly exact (within numerical accuracy) quantum Monte Carlo (QMC) calculations for the interacting homogeneous electron gas (HEG) at various densities ρ^{hom} . For an homogeneous electron gas with homogeneous ionic positive background, the Hartree and electron-ion energies cancel exactly. The calculated QMC total energy $E^{QMC}[\rho^{hom}]$ contains thus the kinetic energy T and the $(E^{ee} - J)$ electron-electron interaction beyond the Hartree term. Subtracting now the kinetic energy $T^0[\rho^{hom}]$ for the non-interacting electron gas of same density, as given exactly by the Thomas-Fermi expression, one obtains straightforwardly

$$e_{XC}(\rho(\mathbf{r})) = \frac{E^{QMC}[\rho^{hom}] - T^0[\rho^{hom}]}{N} \quad \text{with} \quad \rho^{hom} = \rho(\mathbf{r})$$

with N the number of electrons for which the total energy is calculated in the QMC simulation and $\rho^{hom} = V/N$. One may further subtract the exact exchange energy, namely the total energy of the HEG in the Hartree-Fock approximation where the many-body wavefunction is described by a single Slater determinant. This is a famous calculation performed by Dirac in 1930 [7], yielding for the HEG exchange-energy

$$\frac{E_X}{N} = -\frac{3k_F}{4\pi} \simeq \frac{-0.458}{r_s} \text{ a.u.} \quad \text{with} \quad \frac{V}{N} = \frac{4}{3}\pi r_s^3,$$

with r_s the Wigner-Seitz radius, namely the radius of the sphere with volume V/N . Such an expression can alternatively be expressed as a function of the electronic density, yielding the Dirac exchange expression

$$E_X^{Dirac} = -C_X \int d\mathbf{r} \rho(\mathbf{r})^{4/3} \quad \text{with} \quad C_X = \frac{3}{4} \left(\frac{3}{\pi} \right)^{1/3}.$$

By subtraction, one obtains the correlation-only energy per electron $e_C^{hom}(\rho)$. The QMC data points have been fitted by clever functional forms (Vosko-Wilk-Nusair [8], Perdew-Zunger [9], etc.) that are used nowadays in standard DFT codes. We leave this section by noting that for the HEG with cancelling Hartree and electron-ion interactions, the kinetic and exchange energies add up to

$$E_{HEG}^{HF} = \frac{1.105}{r_s^2} - \frac{0.458}{r_s} \quad (\text{a.u.})$$

Without the exchange term, the HEG is unstable with no finite equilibrium r_s value.

Once the exchange-correlation energy is defined, one can proceed with solving the Kohn-Sham equations associated with the fictitious non-interacting electron gas

$$\left(-\frac{\nabla^2}{2} + v^{\text{eff}}(\mathbf{r})\right) \phi_n(\mathbf{r}) = \varepsilon_n \phi_n(\mathbf{r}) \quad \text{with} \quad v^{\text{eff}}(\mathbf{r}) = v^{\text{ions}}(\mathbf{r}) + V^H(\rho(\mathbf{r})) + V^{\text{XC}}(\rho(\mathbf{r})),$$

where we use the LDA exchange-correlation potential $V_{LDA}^{\text{XC}}(\rho(\mathbf{r})) = \partial E_{XC}^{\text{LDA}}(\rho(\mathbf{r}))/\partial \rho(\mathbf{r})$. Solving the Kohn-Sham equations yields the Kohn-Sham electronic energy levels $\{\varepsilon_n\}$ and the Kohn-Sham eigenstates $\{\phi_n\}$ from which the ground-state density and associated LDA total energy can be obtained

$$\begin{aligned} \rho(\mathbf{r}) &= \sum_{n=1}^N |\phi_n(\mathbf{r})|^2 \quad \text{and} \quad T^0 = \sum_{n=1}^N \langle \phi_n | -\nabla^2/2 | \phi_n \rangle \\ E_0^{\text{LDA}} &= T^0 + \int d\mathbf{r} v^{\text{ions}}(\mathbf{r})\rho(\mathbf{r}) + E^H[\rho] + E_{LDA}^{\text{XC}}[\rho] \end{aligned}$$

where the sum extends over the N lowest energy levels (ground-state at zero temperature). An important aspect of such equations is that they are self-consistent: to obtain the $\{\phi_n\}$ one needs to solve the Kohn-Sham equations with a potential that depends *via* the density on ... the $\{\phi_n\}$! In practice, one takes some guess input density ρ_0 , such as a simple superposition of tabulated atomic densities, to build an input XC potential $V_{LDA}^{\text{XC}}(\rho_0(\mathbf{r}))$ that allows obtaining a first guess of Kohn-Sham orbitals. These orbitals allow to build an updated electronic density and a related updated XC potential and Kohn-Sham Hamiltonian, leading to a updated set of orbitals and density. When the input and output electronic densities and/or XC potentials are the same, the self-consistent cycle is stopped, leading to the ground-state self-consistent density and total energy. The technicalities of converging to the correct energy minimum (are there local minima?) and of the convergence rate are difficult issues not dealt with here.

4.2 Structural properties within LDA: average impressive results

We now know how to calculate in practice the ground-state energy within the LDA approximation for a given system characterized by ionic positions and nuclear charges (defining the v^{ion} potential) and the number N of electrons. We thus can, in particular, answer the important question: how good is the LDA approximation? We must remember here that what we are targeting with DFT are the ground-state total energy and charge density. Other observables, such as electronic energy levels, are not *in principle* within the scope of what DFT is designed for.

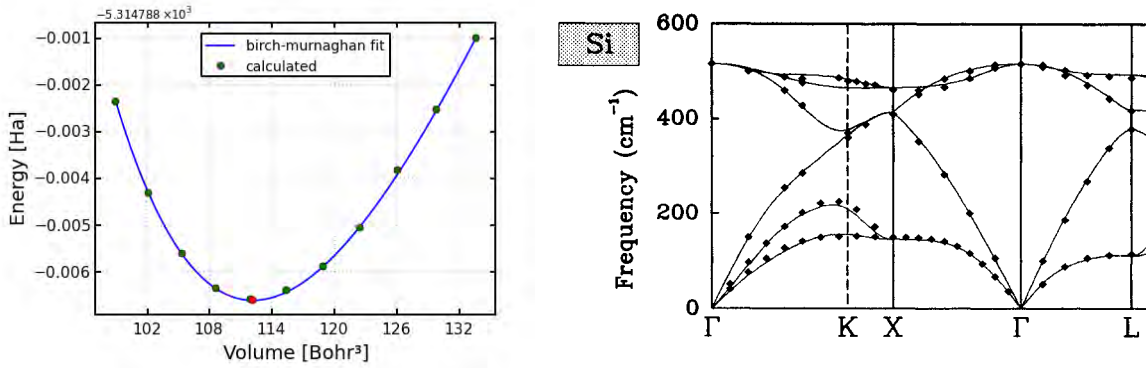


Fig. 1: (Left) Energy versus unit-cell volume for silver. DFT energy data points are fitted by some clever functional form (Birch-Murnaghan fit). The energy minimum gives the equilibrium volume and related lattice parameter as well as interatomic distances that can be compared to experiment (courtesy <http://exciting-code.org/beryllium-volume-optimization-for-cubic-systems>). (Right) Calculated LDA versus experimental phonon dispersion for silicon (from Ref. [13]).

We will come back to that point in the following Sections. In their original papers, Hohenberg, Kohn, and Sham were actually critical about the potential success of the LDA, concluding that for actual systems variations of the charge density were so strong that a model exact in the limit of homogeneous distribution of charges appeared to have little chance of being successful.

We now present in Fig. 1 (left) the results of a standard numerical exercise consisting in finding the equilibrium cell volume (or lattice parameter) for a solid using DFT (here silver in its FCC structure). With the space group known, one can calculate the DFT total energy for various unit cell volumes. The resulting calculated data points can be fitted by some polynomial law (or a more adapted functional form such as the Birch-Murnaghan law), yielding the equilibrium volume at zero temperature for a given approximation to the XC potential. The associated error for several functionals and several crystal families (metals, non-metals) are given in Table 1. Considering non-metallic structures, that include typical covalent systems such as silicon and diamond with very inhomogeneous density distributions, one finds that LDA predicts the lattice

	Metals(14)				Nonmetals (10)			
	LDA	PBEsol	PBE	TPSS	LDA	PBEsol	PBE	TPSS
ME (Å)	-0.136	-0.039	0.046	0.039	-0.042	0.026	0.085	0.066
MAE (Å)	0.136	0.042	0.060	0.060	0.042	0.026	0.085	0.066
MRE (%)	-2.71	-0.76	0.95	0.74	-0.86	0.56	1.76	1.35
MARE (%)	2.71	0.83	1.24	1.15	0.86	0.56	1.76	1.35

Table 1: Statistical data: mean error, mean absolute error, mean relative error MRE % and mean absolute relative error MARE %, for lattice constants Å of a selection of 14 metals and 10 nonmetals. Errors with respected to experimental data corrected for ZPAE (zero point anharmonic expansion) contribution. The PBEsol functional is a modification of PBE for solids [10] while TPSS is a “metaGGA” functional [11] with a dependence on the density but also the Laplacian $\nabla^2 \rho(\mathbf{r})$ proportional to the kinetic energy (adapted from Table IV from Ref. [12]).

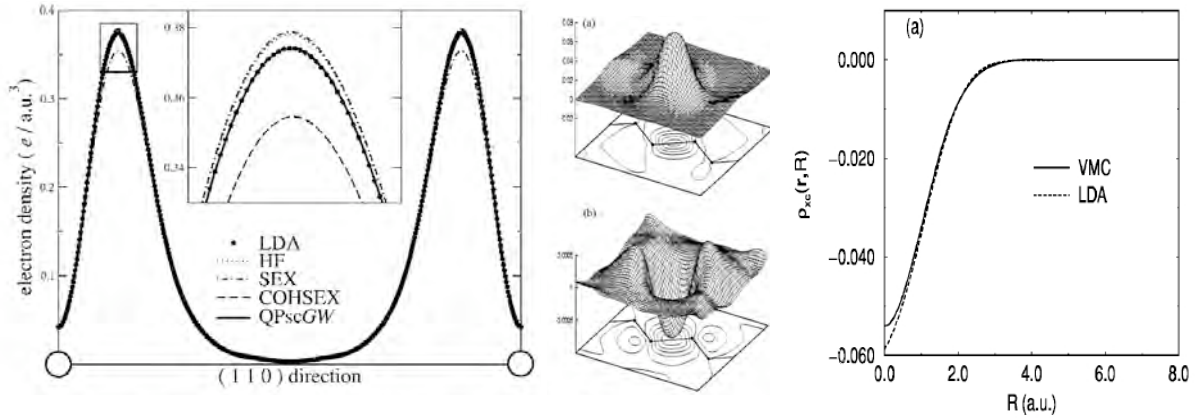


Fig. 2: (Left) Charge density for solid argon along an interatomic bond comparing LDA with the so-called quasiparticle self-consistent QPscGW approximation (from Ref. [14]). (Center and Right) LDA versus variational Monte Carlo (VMC) one-body density matrix and spherically averaged XC hole $\rho_{XC}(\mathbf{r}; R)$ for Silicon (from Ref. [15]).

parameters of solids with an average accuracy well within 1% (see boxed numbers). This is a remarkable results for an approach that is very simple and relies on a approximation assumed to be valid only for systems with homogeneous charge densities (e.g. alkali metals). The error is further systematic, with a tendency to overbind (too small lattice parameters). Such performance can certainly explain the success of DFT combined with the Kohn-Sham formalism and the local density approximation.

Beyond lattice parameters, we further plot in Fig. 1 (right) the LDA phonon band-structure for silicon as compared to experiment [13], with phonon energies standing as 2nd-order derivatives of total energies with respect to ionic positions via the force-constant matrix. Again, the agreement is very remarkable for a system far from displaying a homogeneous charge density. Since the DFT is designed to provide ground-state electronic densities, we now reproduce in Fig. 2 (left) the density of solid argon along a bond direction, comparing the LDA electronic density with results of a self-consistent many-body Green's function approach labeled the QPscGW formalism [14]. Clearly, the agreement is excellent, even in the present case of a very inhomogeneous density profile. Similar results are obtained for the one-body density matrix in Fig. 2 (center) in the case of silicon, comparing now the LDA density matrix built from the Kohn-Sham eigenstates: $\gamma_1(\mathbf{r}, \mathbf{r}') = \sum_{n=1}^N \phi_n(\mathbf{r})\phi_n(\mathbf{r}')$ with a variational Monte Carlo (VMC) reference: $\gamma_1(\mathbf{r}, \mathbf{r}') = N \int d\mathbf{r}_2 \cdots d\mathbf{r}_N \psi^*(\mathbf{r}, \mathbf{r}_2 \cdots \mathbf{r}_N)\psi(\mathbf{r}', \mathbf{r}_2 \cdots \mathbf{r}_N)$. The deviation between the two calculations is well within 1% again.

4.3 LDA satisfies the exchange-correlation sum-rule

This somehow unexpected success of the LDA for systems displaying strongly inhomogeneous charge density distributions relies in particular on the facts that (a) the exchange-correlation (XC) energy depends on a Coulomb-weighted spherical average over the XC-hole and (b) the LDA XC hole satisfies the exchange-correlation sum-rule. Taking the relation between the

electron-electron XC energy and the XC hole, one obtains indeed

$$E_{XC} = \frac{1}{2} \int d\mathbf{r} \rho(\mathbf{r}) \int_0^{+\infty} 4\pi R dR \rho_{XC}^{SA}(\mathbf{r}, R) \quad \text{and} \quad \rho_{XC}^{SA}(\mathbf{r}, R) = \frac{1}{4\pi} \int_{|\mathbf{r}-\mathbf{r}'|=R} d\mathbf{r}' \frac{\rho_{XC}(\mathbf{r}, \mathbf{r}')}{|\mathbf{r}-\mathbf{r}'|}$$

with $\rho_{XC}^{SA}(\mathbf{r}, R)$ the spherically averaged XC-hole around the \mathbf{r} -point using the Coulomb norm. We plot in Fig. 2 (right) such a spherically-averaged XC-hole, comparing again LDA and VMC in the case of Silicon. While for a given $(\mathbf{r}, \mathbf{r}')$ pair of positions the LDA and VMC XC hole differ significantly, their spherically averaged values are remarkably close. Further, it can be shown [16] that the LDA XC hole satisfies an exact sum rule, namely

$$4\pi \int R^2 dR \rho_{XC}^{SA}(\mathbf{r}, R) = -1$$

indicating that if the LDA XC-hole is too small for a given R value, then it is too large in compensation for another R distance. Such properties are very strong desirable constraints that may explain the success of the LDA and ... the failure of subsequent approximations. The inclusion of some kinetic energy ($T-T_0$) in the definition of the DFT XC energy leads to caution when defining the DFT XC hole within what is called the ‘‘adiabatic connection formalism’’ that builds a connection between the non-interacting and interacting systems sharing the same density.

4.4 Jacob’s ladder of functionals: towards accuracy heaven?

Improving on the LDA approximation for a better description of observables related to the total energy (binding energy, atomization energy, structural phase diagrams, activation barriers, elastic constants, phonon spectra, etc.) remains the central issue in the field of DFT. Roughly speaking, two strategies can be followed: the first is to develop functionals that satisfy exact mathematical relations, such as satisfying the XC hole sum rule. The second strategy is more pragmatic and consists in fitting some general functional form with parameters on experimental data. An interesting article recently published by Perdew and coworkers in the journal *Science* and entitled ‘‘Density functional theory is straying from the path toward the exact functional’’ [17] provides a nice discussion on the two philosophies, illustrating further the ‘‘jungle’’ of functionals that exist nowadays. Clearly, functionals fitted to experimental data can be very accurate, but go away from the *ab initio* or first-principles character of DFT.

Concerning the strategy that consists in satisfying exact relations, an interesting illustration can be found in the early days of the so-called gradient corrected functionals that attempt to go away from the local density approximation by devising functionals that depend not only on the local density but also on its gradient to capture some information about charge inhomogeneities. Early functionals with low-order gradient corrections (LGC), such as the following one for the exchange (X) energy (σ the spin degree of freedom)

$$E_X^{LGC} = E_X^{LDA} - \beta \sum_{\sigma} \int d\mathbf{r} \rho_{\sigma}^{4/3} x_{\sigma}^2 \quad \text{with} \quad x_{\sigma} = \frac{|\nabla \rho_{\sigma}|}{\rho_{\sigma}^{4/3}} \quad \text{a-dimensional}$$

really failed in improving over the LDA. In fact, E_X^{LGC} does not satisfy the exchange-hole sum rule, leading to a divergency in the vacuum where $\rho(\mathbf{r})$ decays exponentially, etc. Further, the potential felt by an electron far away from an atom, molecule, surface, etc. should scale as $-1/r$. This term comes from the exchange potential, yielding for the exchange energy density at long distance in the vacuum

$$\lim_{r \rightarrow \infty} \epsilon_X(\mathbf{r}) \simeq -\frac{\rho(\mathbf{r})}{2r} \quad \text{with} \quad \rho(\mathbf{r}) = 2\rho_{\uparrow}(\mathbf{r}) = 2\rho_{\downarrow}(\mathbf{r}) \quad (\text{unpolarized systems}).$$

To cure such problems, Becke proposed in 1988 an exchange functional (B88) [18] that scales smoothly between the small and large $x_{\sigma} = |\nabla\rho_{\sigma}|/\rho_{\sigma}^{4/3}$

$$E_X^{B88} = E_X^{LDA} - \beta \sum_{\sigma} \int d\mathbf{r} \rho_{\sigma}^{4/3} \frac{x_{\sigma}^2}{1 + 6\beta \sinh^{-1}(x_{\sigma})} \quad (\beta \text{ parameter}).$$

The GGA correction vanishes for small gradients ($x_{\sigma} \rightarrow 0$). With $\rho(\mathbf{r}) \simeq e^{-\alpha r}$ for large r , $x_{\sigma} \rightarrow e^{\alpha r/3}$, and $\sinh^{-1}(x_{\sigma}) \rightarrow \alpha r/3$, the correct (vacuum) asymptotic behavior is recovered. This is the exchange functional used in the celebrated BLYP functional (B=Becke88). Here exact relations (asymptotic behavior, low or high density limit, sum rules, etc.) lead to a functional form that still contains one parameter fitted to experimental data, combining *de facto* the two above-mentioned strategies. Such generalized gradient approximations (GGA) constitute the “second rung” of the so-called Jacob’s ladder of functionals that provides a classification of functionals with increasing average accuracy [19]. Well known functionals of that family include the PW91 (Perdew-Wang 1991) [20], the PBE (Perdew-Becke-Ernzherof) [21], or the BLYP (Becke-Lee-Yang-Parr) functionals [22]. As can be seen in Table 1, the PBE functional leads to better results for metals as compared to the LDA, with a tendency to underbind (too large lattice parameters), but no improvements for non-metallic systems (e.g. semiconductors). We witness here the fact that functionals developed for finite size systems, with, e.g., the proper treatment of long-range behavior in the vacuum, may not be relevant for solids where there is ... no vacuum. The PBEsol functional (see Table 1) is a modification of PBE for solids, yielding better results indeed for periodic extended systems.

We now introduce a key generalization of DFT, namely the merging of DFT and Hartree-Fock yielding “hybrid functionals” where density-dependent expressions are complemented by one-body-orbital dependent exact exchange. For the Kohn-Sham system, we indeed know how to calculate the “exact” exchange energy “associated with” the Kohn-Sham eigenstates $\{\phi_n\}$

$$E_X = -\frac{1}{2} \sum_{ij}^{occ} \iint d\mathbf{r} d\mathbf{r}' \frac{\phi_i^*(\mathbf{r})\phi_j(\mathbf{r})\phi_j^*(\mathbf{r}')\phi_i(\mathbf{r}')}{|\mathbf{r} - \mathbf{r}'|} \delta_{\sigma_i\sigma_j},$$

where we have re-introduced the spin variables. This is more expensive than pure density functionals (Hartree-Fock (HF) scales as N^4 with system size) but helps in several directions:

- it offers clearly the correct asymptotic behavior for the electronic potential in the vacuum and satisfies the exchange-hole sum rule

- it helps curing *the self-interaction (SI) problem*: within DFT, since the charge density depends on the occupied orbitals, the action of $v^{\text{eff}}[\rho]$ on an occupied orbital amounts to having an electron interacting with itself (consider the H atom system!). This is a dramatic problem for localized orbitals. It does not exist within HF since the SI in the Hartree and exchange energies cancel out.

However, mixing 100% of exact exchange with a density dependent correlation functional leads (in general) to a failure. Density-dependent XC functionals are usually built together for reproducing the total XC potential properties. Namely, they benefit from large error cancellations. Considerations built on the “adiabatic connection” between the non-interacting and interacting electronic systems generated the historical Becke half-and-half functional: $E^{XC} = 0.5E^X(HF) + 0.5E^X(\text{Slater}) + E^C(\text{LYP=Lee-Yang-Parr})$. With a fitting strategy on 56 small molecules atomization energies, 8 proton affinities, and 10 first-row total atomic energies, the “Becke 3 parameters” (the B3 of B3LYP) exchange functional [23] mixes Slater LDA and B88 GGA exchange with 20% of exact exchange. Using perturbation theory, Perdew, Burke and Ernzerhof advocated 25% of exact exchange, leading to the 1996 PBE0 functional [24]. The B3LYP and PBE0 formula are probably the most popular functionals in quantum chemistry for finite size systems.

To combine the need for having 100% of exact exchange in the long-range in the case of finite size systems, while a much smaller amount of exchange in the short-range, range-separated hybrids were introduced [25]. The idea is to define a short-range (SR) and long-range (LR) Coulomb interaction thanks, e.g., to the error function erf, allowing the introduction of a long-range-only exchange potential

$$v_X^{LR}(\mathbf{r}, \mathbf{r}'; \omega) = - \sum_i^{\text{occ}} \phi_i(\mathbf{r}) \phi_i^*(\mathbf{r}') \frac{\text{erf}(\omega|\mathbf{r} - \mathbf{r}'|)}{|\mathbf{r} - \mathbf{r}'|}.$$

The use of the complementary error function allows to introduce a short-range-only exact exchange. As such, one can introduce different amounts of local (Dirac) and exact exchange in the short and long ranges. The ω parameter controls the (inverse) effective length that partition the interaction between short or long range. The very popular CAM-B3LYP functional [26] includes 65% of LR exact exchange with $\omega = 0.33$ while the LC- ω PBE includes 100% of LR exact exchange with $\omega = 0.4$.

We abandon here the hope to provide a thorough description of functionals. Let’s conclude on the fact that contrary to finite size molecules, long-range Coulomb interactions in solids are renormalized by the macroscopic dielectric constant ϵ_M that diverges in the case of metallic systems. As such, the long-range amount of exact exchange in solids should be qualitatively proportional to $(1/\epsilon_m)$, and even exponentially decaying in metals (Yukawa-type behavior). This is, e.g., the rationale behind the HSE functional, a range-separated hybrid for extended systems relying on the solid-state physics language of screened Coulomb potentials [27].

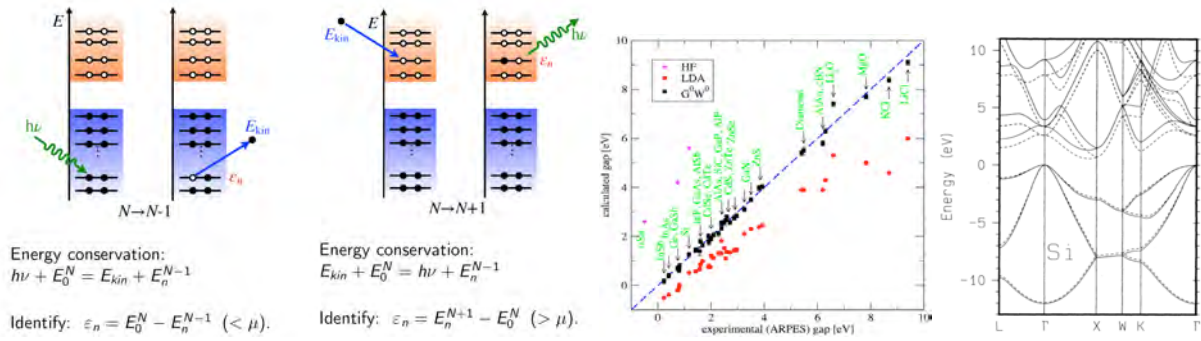


Fig. 3: (Left) Symbolic representation of direct and inverse photoemission experiments interpreted from the standard “one-electron energy levels” diagram. (Center) Compilation of LDA band gaps (red dots) in semiconductors and insulators as compared to experiments (first diagonal), Hartree-Fock data (cyan dots), and to a higher-level many-body Green’s function approach, the so-called $G_0W_0@LDA$ formalism (courtesy Valerio Olevano). (Right) LDA (dashed) versus GW (full lines) band-structure of Silicon. The zero of energy has been set to the valence bands top (from Ref. [28]).

5 On the meaning of Kohn-Sham auxiliary 1-body eigenstates

We tackle now a delicate problem within DFT, namely that of electronic properties. As discussed above, DFT is a ground state formalism designed to reproduce ground-state total energies and electronic density. As such, it is not designed to provide electronic energy levels. However, there is a very large literature exploiting Kohn-Sham eigenvalues for plotting the band-structure of realistic materials, with much success in many situations, but also well-documented limitations and failures. These are such aspects that we briefly explore now.

The meaning of what we call “electronic energy levels” when we plot a band-structure (or discrete energy levels in the case of a molecule) must be found in the experiment used to measure them, e.g., a photoemission experiment. In direct photoemission (see Fig. 3 (left)), a photon with energy $h\nu$ arrives on a piece of matter in its ground-state (with energy $E_0[N]$) and ejects an electron with some residual kinetic energy E_{kin} , leaving the system with $(N-1)$ electrons and an energy $E_n[N-1]$. The index n labels an eigenstate of the $(N-1)$ electron system. We define the energy of the electron in the system as $\varepsilon_n = E_0[N] - E_n[N-1]$, the energy of the level from which the electron was ejected. Using conservation of energy, $E_0[N] - E_n[N-1] = E_{kin} - h\nu$ measured experimentally. Similar considerations can be used to assimilate in inverse photoemission the differences of energy ($E_n[N+1] - E_0[N]$) between an excited state of the $(N+1)$ -electron system and the ground-state of the N -electron system as the unoccupied level energies.

Electronic energy levels as measured experimentally using photo-emission experiments are really differences of total energies between excited states of the $(N+1)$ or $(N-1)$ electron systems and the N -electron system in its ground state, namely $\varepsilon_n = E_n[N+1] - E_0[N]$ for unoccupied levels and $\varepsilon_n = E_0[N] - E_n[N-1]$ for occupied levels. What is the relation between the $\{\varepsilon_n^{KS}\}$ Kohn-Sham eigenvalues and such total energy differences between charged and neutral systems?

5.1 The band gap problem with DFT Kohn-Sham eigenvalues

Before trying to find a rationale for the Kohn-Sham energy levels, namely the energy of the fictitious independent electrons in the effective potential v^{eff} defined above, let's consider actual calculations, starting with the band gap of standard semiconductors and insulators. Data are compiled in Fig. 3 (center). The results of actual DFT calculations using the LDA XC potential (red dots) drive us to the conclusion that the band structure obtained with Kohn-Sham eigenvalues yields too small gaps. In the DFT Kohn-Sham world, the band gap of silicon turns to be about 0.5-0.6 eV, a factor two smaller than the 1.2 eV experimental value. Very similar results are obtained using “pure” DFT functionals, namely functionals not including some amount of exact exchange such as PBE. This is the band gap problem within DFT. A close inspection of Fig. 3 (center) for small gap systems further reveals that some systems, that are gaped semiconductors experimentally, turn out to be metallic (negative gap, namely an overlap of the occupied and empty bands) within LDA. This is the case, e.g., of the simple germanium system. It is fair to say that turning an insulator into a metal is a somehow dramatic failure. This tendency to underestimate band gaps can also be witnessed in the case of organic molecules for which the Kohn-Sham LDA HOMO-LUMO (highest occupied/lowest unoccupied molecular orbitals) energy gap can be underestimated by several eVs as compared to experiment or higher level techniques (see Fig. 4 (left)).

To better understand why DFT is still very widely used to study the electronic properties of a large variety of systems, we provide now in Fig. 3 (right) the LDA band structure for silicon (dashed line) that we compare to a much more accurate many-body perturbation theory approach, the *GW* formalism. We align the two band structures at the top of the valence band (zero of energy). The remarkable feature evidenced by this plot is that besides the band gap problem, the dispersion of bands in the valence and conduction manifolds are extremely close. Namely, the two band-structures could agree very well if a “scissor” operation, consisting in rigidly shifting the conduction bands by 0.5-0.6 eV higher in energy, is applied.

Contrary to Kohn-Sham DFT, Hartree-Fock (HF) yields too large gaps (see cyan dots in Fig. 3 (center) and HF data in Fig. 4 (left)). In the HF world, the band gap of Silicon is of the order of 6 eV, dramatically too large. This is due to the lack of correlations. Clearly, mixing some amount of exact exchange with DFT density-dependent XC potentials leads to much better gaps. This is exemplified in Fig. 4 (left) with the B3LYP data that are in better agreement with experiment. This is a clear incentive to mix exact exchange and density-dependent functionals, namely to use hybrid functionals for electronic properties, even though the criteria for selecting the proper amount of exact exchange for a given system is a difficult challenge if one wishes to preserve an *ab initio* (no fitting parameters) approach. The B3LYP functional includes 20% of exact exchange, an amount that does not seem sufficient to provide an accurate gap.

The band gap problem in DFT has been analyzed in depth and is related to the lack of a discontinuity of density-based XC potentials upon addition or removal of an electron [33, 34]. In a typical bulk system composed of the order of 10^{23} electrons per cm^3 , adding or removing an electron delocalized in some Bloch state hardly changes the charge density. As such, an

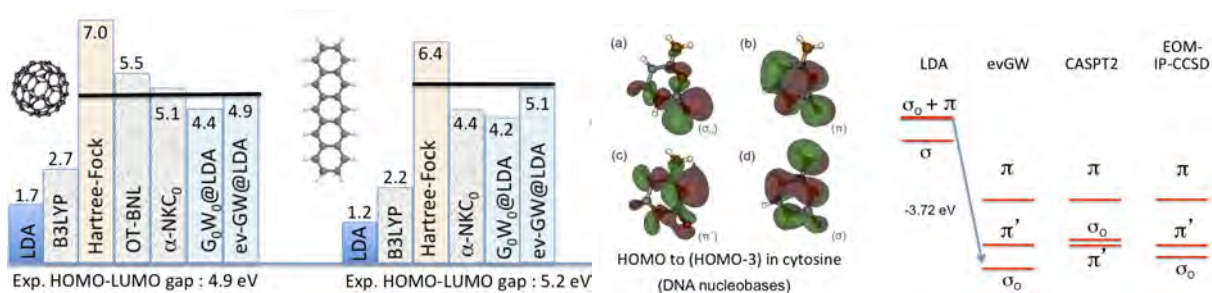


Fig. 4: (Left) HOMO-LUMO gap of gas phase (isolated) C_{60} fullerene and pentacene molecules. Various DFT and generalized DFT formalisms, including Kohn-Sham LDA, Hartree-Fock, B3LYP hybrid functionals, optimally-tuned range-separated hybrid (OT-BNL; Ref. [29]) or Koopmans' compliant (KNC; Ref. [30]) functionals are compared to many-body perturbation theories (G_0W_0 and evGW approaches) and to experiment (horizontal black line). (adapted from Ref. [31]) (Right) Top-most occupied levels for isolated cytosine DNA nucleobases as calculated using Kohn-Sham LDA approach and higher level many-body perturbation theories (evGW, CASPT2, EOM-IP-CCSD). Notice the reordering of levels from LDA to higher level approaches (adapted from Ref. [32]).

exchange-correlation potential built as a functional of the charge density will show no variations upon, e.g., adding an electron that will populate the bottom of the conduction bands across the gap. A simple analysis of the exact exchange operator clearly reveals that the XC potential should be discontinuous upon adding a charge to the neutral system.

We conclude this section with a warning: as discussed above, the DFT Kohn-Sham approach may turn a very standard band semiconductor, such as germanium, into a metal. This does not mean that the “band structure picture” fails and that strong correlations beyond mean-field (Mott transition) should be invoked to describe germanium. It just means that the DFT Kohn-Sham formalism with local functionals of the electronic density is not an accurate, not even a well-defined, formalism to capture band gaps.

5.2 Level ordering and self-interaction problems

This simple analysis in terms of band gap errors that can be cured by a rigid shift of, e.g., empty states needs however to be taken with care. While silicon and other simple sp -bonded semiconductors or insulators are characterized by Bloch states displaying equivalent spatial localization properties, systems mixing localized and extended states may suffer from a wrong ordering of levels at the Kohn-Sham DFT level with density-dependent functionals. Such systems include, e.g., transition metals displaying localized $3d$ levels together with itinerant (delocalized) sp bands, surfaces with extended bulk states versus localized surface states, or modern molecular electronic devices with extended states in the metallic electrodes but very localized molecular states in the junction. In the case of occupied levels, the self-interaction problem discussed above in Section 4.4 affects the localized states much more than the delocalized ones. As such, the ordering of levels within the occupied manifold can be wrong as well within DFT Kohn-Sham. This is exemplified in Fig. 4 (right) in the case of the gas phase (isolated) cytosine DNA

nucleobasis: while the highest occupied molecular orbital should be a delocalized π orbital, the Kohn-Sham LDA approach predicts erroneously at the top of the occupied manifold a very localized σ_O molecular orbital, localized on the oxygen. The self-interaction error is erroneously repelling high in energy this localized σ_O orbital. Hybrid functionals, with a portion of exact exchange, help in curing this problem since Hartree-Fock is self-interaction free.

5.3 What is the meaning of Kohn-Sham eigenvalues?

We now turn to a more formal analysis of the meaning of Kohn-Sham eigenvalues. We start by recovering the Kohn-Sham eigenvalue equation using the variational principle for the ground-state energy considered as a functional of the one-body Kohn-Sham auxiliary eigenstates $\{\phi_n\}$. We thus define a Lagrangian

$$\Omega[\{\phi_i\}, \{\lambda_{ij}\}] = E[\{\phi_i\}] + \sum_{i \leq j} \lambda_{ij} \left(\delta_{ij} - \langle \phi_i | \phi_j \rangle \right),$$

where the $\{\lambda_{ij}\}$ are the Lagrange parameters insuring that the $\{\phi_n\}$ are kept orthonormalized in the minimization process. The minimization of $\Omega[\{\phi_i, \lambda_{ij}\}]$ with respect to some $\phi_i^*(\mathbf{r})$ leads to

$$\left(-\frac{\nabla^2}{2} + v^{\text{eff}}(\mathbf{r}) \right) \phi_i(\mathbf{r}) = \sum_j \lambda_{ij} \phi_j(\mathbf{r}) \quad \text{with} \quad v^{\text{eff}}(\mathbf{r}) = v^{\text{ion}}(\mathbf{r}) + V^H(\rho(\mathbf{r})) + V^{\text{XC}}(\rho(\mathbf{r})),$$

using, e.g., the following chain rule for density-dependent potentials

$$\frac{\partial}{\partial \phi_i^*(\mathbf{r})} = \frac{\partial}{\partial \rho(\mathbf{r})} \times \frac{\partial \rho(\mathbf{r})}{\partial \phi_i^*(\mathbf{r})} = \frac{\partial}{\partial \rho(\mathbf{r})} \times \phi_i(\mathbf{r}).$$

A unitary rotation that diagonalizes the λ_{ij} matrix allows to recover the standard Kohn-Sham eigenvalue equation postulated in Section 3.4. However, we understand here that the Kohn-Sham eigenvalues are just Lagrange multipliers and their relation with addition/removal energies, as defined in a photoemission experiment, is far from clear! As another indication of the difficulty in identifying Kohn-Sham eigenvalues with total-energy differences between the neutral and charged systems, let's consider now the sum of Kohn-Sham eigenvalues over occupied states, namely

$$\sum_{i=1}^N \varepsilon_n = \sum_{i=1}^N \langle \phi_i | -\nabla^2/2 + v^{\text{eff}}(\mathbf{r}) | \phi_i \rangle = T_0 + \int d\mathbf{r} \left(v^{\text{ion}}(\mathbf{r}) + V^H(\mathbf{r}) + V^{\text{XC}}(\mathbf{r}) \right) \rho(\mathbf{r})$$

to be compared to the ground-state total energy

$$E[N] = T_0 + \int d\mathbf{r} v^{\text{ion}}(\mathbf{r}) \rho(\mathbf{r}) + J[\rho] + E^{\text{XC}}[\rho] \quad \text{with} \quad J[\rho] = \frac{1}{2} \int d\mathbf{r} V^H(\mathbf{r}) \rho(\mathbf{r}).$$

As a result, the ground-state total energy for, e.g., the N -electron system reads also

$$E[N] = \sum_{i=1}^N \varepsilon_n - J[\rho] + E^{\text{XC}}[\rho] - \int d\mathbf{r} V^{\text{XC}}(\mathbf{r}) \rho(\mathbf{r}) \quad \text{with} \quad V^{\text{XC}}(\mathbf{r}) = \frac{\partial E^{\text{XC}}[\rho]}{\partial \rho(\mathbf{r})},$$

where the sum of occupied level energies are completed by electron interaction terms. As such, differences of total energies such as $E[N+1] - E[N]$ cannot be identified simply to individual Kohn-Sham eigenstates and the meaning of Kohn-Sham eigenstates remains elusive.

5.4 Janak theorem and fractional occupations in ensemble DFT

Janak theorem [35] is an important relation that may pave the way to progress in the use of DFT to tackle not only ground-state total energies but also electronic excitations. The seminal idea is a generalization of the Kohn-Sham formalism to *fractional occupation numbers* of the electronic energy levels $\{\varepsilon_n\}$. In the standard Kohn-Sham approach, occupation numbers were set to unity below the Fermi level and zero above (zero temperature). In the generalized fractional approach, the kinetic energy and electronic density read

$$T_J[\rho] = \sum_i n_i \langle \phi_i | -\nabla^2/2 | \phi_i \rangle \quad \text{and} \quad \rho(\mathbf{r}) = \sum_i n_i |\phi_i(\mathbf{r})|^2,$$

where the index J stands for Janak. As such, the total energy is not only a functional of the one-body orbitals $\{\phi_n\}$, but also of the fractional occupations $\{n_i\}$ as additional variational parameters, namely

$$E_{GS} = \min_{\phi_i, n_i} E[\{n_i, \phi_i\}] \quad \text{with} \quad E = T_J[\{n_i, \phi_i\}] + \int d\mathbf{r} v^{ion}(\mathbf{r}) \rho(\mathbf{r}) + J[\rho] + E^{XC}[\rho],$$

where $\rho(\mathbf{r}) = \sum_i n_i |\phi_i(\mathbf{r})|^2$. The minimization with respect to the occupation factors leads to the Janak formula

$$\varepsilon_i = \frac{\partial E}{\partial n_i} \quad (\text{Janak formula})$$

telling us that one-body eigenvalues are related to the variation of the total energy with respect to an infinitesimal variation of the population. Since the Kohn-Sham formalism is a reduction of the Janak approach to $n_i = 1$ or $n_i = 0$ for occupied/empty levels, the Kohn-Sham eigenvalues can be interpreted as derivatives of the total energy at occupation numbers taken to be 0 or 1 namely

$$\varepsilon_i^{KS} = \left(\frac{\partial E}{\partial n_i} \right)_{n_i=0 \text{ or } 1}.$$

This differs from the experimental definition that electronic energy levels are variations of the total energy with respect to a unity (not infinitesimal) change of level population.

Apart from the technicalities of the derivation, a central question is related to the meaning of fractional occupations and, more generally, fractional number of electrons. The two concepts are not equivalent. One may consider a situation where fractional occupations are introduced while keeping the number of electrons fixed to N , namely $\sum_i n_i = N$. This is a very natural situation at finite temperature with the Fermi-Dirac distribution. Even at zero temperature, this is just reminiscent of Fermi liquid theory revealing that particle interactions lead to non-integer occupation number close to the Fermi level. On simpler grounds, it is also a useful exercise to consider the 1st-order density matrix

$$\gamma_1(\mathbf{r}, \mathbf{r}') = N \int \dots \int d\mathbf{r}_2 \dots d\mathbf{r}_N \psi(\mathbf{r}, \mathbf{r}_2, \dots, \mathbf{r}_N) \psi^*(\mathbf{r}', \mathbf{r}_2, \dots, \mathbf{r}_N)$$

for which it can be demonstrated that the expression of T and ρ as a function of fractional occupation is exact with the $\{n_i\}$ and $\{\phi_i\}$ the eigenvalues and eigenstates of γ_1 . These eigenstates are called ‘‘natural orbitals’’ and the eigenvalues fulfill $\sum_i n_i = N$.

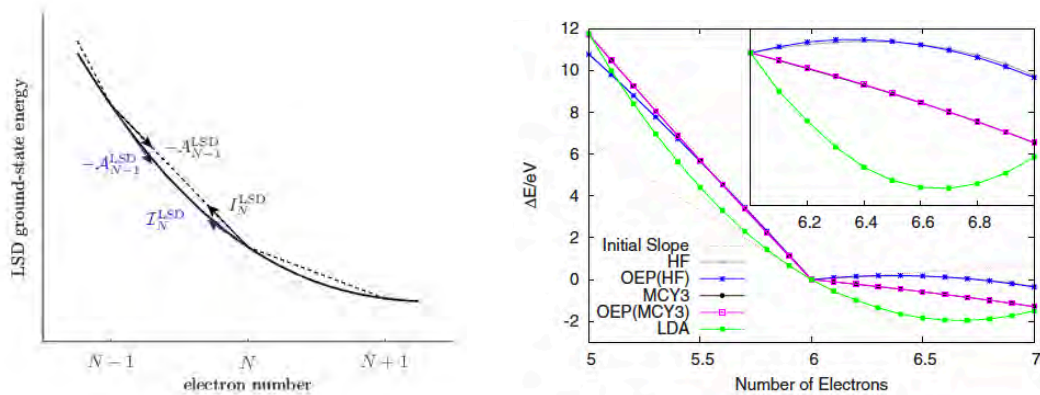


Fig. 5: (Left) Symbolic representation of the exact total energy (dotted lines) and DFT total energy (full line) as a function of the (continuous) electron number. The arrows indicate the right/left energy derivatives at integer values of the number of electrons in relation to the electronic affinity of the $N-1$ electron system (A_{N-1}^{LSD}) and the ionization potential ($\mathcal{I}_N^{\text{LSD}}$) of the N -electron system. In the DFT Kohn-Sham approach, A_{N+1}^{LSD} and $\mathcal{I}_N^{\text{LSD}}$ are taken as the opposite of the LUMO energy of the $N-1$ -electron system and HOMO energy of the N -electron system (from Ref. [30]). (Right) Difference energy of the carbon atom $E = E(N_0 + \delta N) - E(N_0)$ ($N_0 = 6$) with several different functionals using OEP (optimized effective potentials) and GKS (generalized Kohn-Sham). Dotted line follows the initial slope for the non-straight functionals. The inset shows the range $6 < N < 7$ in more detail (from Ref. [39]).

Janak’s theorem considers, however, the second situation where the total number of electrons is fractional, namely N becomes a continuous variable. As such, while photoemission measures how much the total energy changes upon the removal/addition of a full electron, Janak’s theorem provides a relation for the removal/addition of an infinitesimal charge. Such a fractional number of electrons can be rationalized on the basis of the grand-canonical ensemble, namely when the system of interest can exchange electrons with a “bath.” The fractional charge can then be associated with a fractional probability of finding the charge in the (sub)system of interest. In quantum mechanics, this can be described by mixed states, that is a statistical ensemble of pure states. This is the basis for “ensemble DFT” [36, 37] that considers ensemble densities

$$\rho(\mathbf{r}) = (1 - \omega)\langle\psi_1|\hat{\rho}(\mathbf{r})|\psi_1\rangle + \omega\langle\psi_2|\hat{\rho}(\mathbf{r})|\psi_2\rangle,$$

where $|\psi_1\rangle$ and $|\psi_2\rangle$ are distinct many-body eigenstates, e.g., the ground-state and first-excited state of the N -electron system, or the ground-states of the N - and $N+1$ -electrons systems. In the first case, ensemble DFT strives to build a DFT approach to neutral excitations (e.g. optical excitations); in the second one, charged excitations (photoemission) are targeted.

We now summarize the main results associated with the variation of the total ground-state energy with respect to a continuous number of electrons. A first important result is that the total energy should be concave and piecewise linear between two integer values of N [38]. This is represented on the left of Fig. 5 as the dotted lines. We observe in particular that the derivative of the total energy with respect to the number of electrons is discontinuous across an integer value: the left and right derivatives are not identical. The piece-wise linearity on each side of an integer value means in particular that the fractional derivatives and the corresponding differences of total energy between integer N -values are identical.

Let's now turn to pure DFT with XC functionals of the density. It can be shown and confirmed by actual calculations that within DFT, the total energy is a concave and smooth function of the number of electrons (see Fig. 5 (left) full line and Fig. 5 (right) green line). In particular the left and right derivatives at integer values of N are identical and not equal to differences of total energy for integer variations of N . One recovers, in particular, the problem of the lack of discontinuity of the XC potential. As such, following the Janak theorem, the Kohn-Sham eigenvalues cannot be identified with electronic energy levels as measured by photoemission. On the contrary, it is found that the Hartree-Fock energy is a convex function of N with discontinuous derivatives at integer values (blue line Fig. 5 (right)). As such, mixing some DFT local functionals with some amount of exact exchange may result in a close-to-straight-line dependence of the total energy between integer values of N , which is just the condition we need for matching infinitesimal derivatives with total energy differences upon adding/removing an electron. This is yet another rationale for using hybrid functionals. However, which amount of mixing should be used for a given system, is again a difficult question to answer if we do not accept fitting strategies to known experimental data. See, e.g., Ref. [29,30] for a mathematically based strategy avoiding empirically adjusted parameters.

Here again, the hunt for a generalized DFT formalism able to tackle excited properties is an on-going boiling activity. In the case of weakly to moderately correlated systems, rather simple many-body perturbation theories such as the GW formalism, with a limited $\mathcal{O}(N^4)$ scaling with system size, is getting very popular in condensed matter physics and, more recently, quantum chemistry (see Figs. 3 and 4). We emphasize however that even if adopting alternative approaches to DFT, Kohn-Sham $\{\varepsilon_n^{KS}, \phi_n^{KS}\}$ eigenvectors remain very valuable zeroth-order one-body eigenstates to build higher-order correlation operators. In particular, GW calculations start generally with the knowledge of the time-ordered Green's function

$$G(\mathbf{r}, \mathbf{r}'; \omega) = \sum_n \frac{\phi_n^{KS}(\mathbf{r}) \phi_n^{KS,*}(\mathbf{r}')}{\omega - \varepsilon_n^{KS} + i \times \text{sign}(\varepsilon_n^{KS} - E_F) \times 0^+}$$

built with KS eigenstates and of the (RPA) screened Coulomb potential $W = V + V\chi_0 W$ and independent-electron susceptibility χ_0 relying again on Kohn-Sham eigenstates

$$\chi^0(\mathbf{r}, \mathbf{r}'; \omega) = \sum_{nm} (f_n - f_m) \frac{\phi_m^{KS}(\mathbf{r}) \phi_n^{KS,*}(\mathbf{r}') \phi_n^{KS}(\mathbf{r}) \phi_m^{KS,*}(\mathbf{r}')}{\omega - (\varepsilon_n^{KS} - \varepsilon_m^{KS}) + i0^+}$$

with $(f_{n/m})$ occupation factors. Even though DFT Kohn-Sham eigenstates do not represent here the final quantities that will be used to interpret the experimental data, they remain very valuable, representing affordable starting piece of information on the electronic properties.

References

- [1] R.M. Dreizler and E.K.U. Gross: *Density-Functional Theory* (Springer, Berlin, Heidelberg, 1990)
- [2] R.G. Parr and Y. Weitao: *Density-Functional Theory of Atoms and Molecules* (Oxford University Press, 1994)
- [3] P. Hohenberg and W. Kohn, Phys. Rev. **136**, B864 (1964)
- [4] M. Levy, Proc. Natl. Acad. Sci. USA **76**, 6062 (1979)
- [5] W. Kohn and L.J. Sham, Phys. Rev. **140**, A1133 (1965)
- [6] D.M. Ceperley and B.J. Alder, Phys. Rev. Lett. **45**, 566 (1980)
- [7] P.A.M. Dirac, Proc. Camb. Phil. Soc. **26**, 376 (1930)
- [8] S.H. Vosko, L. Wilk, and M. Nusair, Can. J. Phys. **58**, 1200 (1980)
- [9] J.P. Perdew and Alex Zunger, Phys. Rev. B **23**, 5048 (1981)
- [10] J.P. Perdew, A. Ruzsinszky, G.I. Csonka, O.A. Vydrov, G.E. Scuseria, L.A. Constantin, X. Zhou, and K. Burke, Phys. Rev. Lett. **100**, 136406 (2008)
- [11] J. Tao, J.P. Perdew, V.N. Staroverov, and G.E. Scuseria, Phys. Rev. Lett. **91**, 146401 (2003)
- [12] G.I. Csonka *et al.*, Phys. Rev. B **79**, 155107 (2009)
- [13] P. Giannozzi, S. de Gironcoli, P. Pavone, and S. Baroni, Phys. Rev. B **43**, 7231 (1991)
- [14] F. Bruneval, N. Vast, and L. Reining, Phys. Rev. B **74**, 045102 (2006)
- [15] P.R.C. Kent, R.Q. Hood, M.D. Towler, R.J. Needs, and G. Rajagopal Phys. Rev. B **57**, 15293 (1998)
- [16] O. Gunnarsson and B.I. Lundqvist, Phys. Rev. B **13**, 4274 (1976)
- [17] M.G. Medvedev, I.S. Bushmarinov, J. Sun, J.P. Perdew, and K.A. Lyssenko, Science **355**, 49 (2017)
- [18] A.D. Becke, Phys. Rev. A **38**, 3098 (1988)
- [19] J.P. Perdew, A. Ruzsinszky, and J. Tao, J. Chem. Phys. **123**, 062201 (2005)
- [20] J.P. Perdew *et al.*, Phys. Rev. B, **46**, 6671 (1992)
- [21] J.P. Perdew, K. Burke, and M. Ernzerhof, Phys. Rev. Lett. **77**, 3865 (1996)
- [22] C. Lee, W. Yang, and R.G. Parr, Phys. Rev. B **37**, 785 (1988)

-
- [23] A.D. Becke, *J. Chem. Phys.* **98**, 5648 (1993)
- [24] C. Adamo and V. Barone, *J. Chem. Phys.* **110**, 6158 (1999)
- [25] T. Leininger, H. Stoll, H.-J. Werner, and A. Savin, *Chem. Phys. Lett.* **275**, 151 (1997)
- [26] H. Iikura, T. Tsuneda, T. Yanai, and K. Hirao, *J. Chem. Phys.* **115**, 3540 (2001)
- [27] J. Heyd and Gustavo E. Scuseria, *J. Chem. Phys.* **118**, 8207 (2003)
- [28] M. Rohlfing, P. Krüger, and J. Pollmann, *Phys. Rev. B* **48**, 17791 (1993)
- [29] S. Refaely-Abramson, R. Baer, and L. Kronik, *Phys. Rev. B* **84**, 075144 (2011)
- [30] I. Dabo, A. Ferretti, N. Poilvert, Y. Li, N. Marzari, and M. Cococcioni, *Phys. Rev. B* **82**, 115121 (2010)
- [31] C. Faber, I. Duchemin, T. Deutsch, C. Attaccalite, V. Olevano, and X. Blase, *J. Matter. Sci.* **47**, 7472 (2012)
- [32] C. Faber, C. Attaccalite, V. Olevano, E. Runge, X. Blase, *Phys. Rev. B* **83**, 115123 (2011)
- [33] J.P. Perdew and M. Levy, *Phys. Rev. Lett.* **51**, 1884 (1983)
- [34] L.J. Sham and M. Schlüter, *Phys. Rev. Lett.* **51**, 1888 (1983)
- [35] J.F. Janak, *Phys. Rev. B* **18**, 7165 (1978)
- [36] A.K. Theophilou, *J. Phys. C* **12**, 5419 (1978)
- [37] E.K.U. Gross, L.N. Oliveira, and W. Kohn, *Phys. Rev. A* **37**, 2809 (1988)
- [38] J.P. Perdew, R.G. Parr, M. Levy, and J.L. Balduz, *Phys. Rev. Lett.* **49**, 1691 (1982)
- [39] A.J. Cohen, P. Mori-Sánchez, and W. Yang, *Phys. Rev. B* **77**, 115123 (2008)